# Rods Contribute to Visual Behavior in Larval Zebrafish

Prahatha Venkatraman,[1,*] Ishara Mills-Henry,[2,†] Karthik Ramaswamy Padmanabhan,[1,‡] Pete Pascuzzi,[3–5] Menna Hassan,[1] Jingyi Zhang,[6] Xinlian Zhang,[7] Ping Ma,[7] Chi Pui Pang,[8,9] John E. Dowling,[2] Mingzhi Zhang,[9] and Yuk Fai Leung[1,10–12]

[1]Department of Biological Sciences, Purdue University, West Lafayette, Indiana, United States
[2]Department of Molecular and Cellular Biology, Harvard University, Cambridge, Massachusetts, United States
[3]Department of Biochemistry, Purdue University, West Lafayette, Indiana, United States
[4]Purdue University Center for Cancer Research, Purdue University, West Lafayette, Indiana, United States
[5]Purdue University Libraries, Purdue University, West Lafayette, Indiana, United States
[6]Center for Statistical Science, Tsinghua University, Beijing, China
[7]Department of Statistics, University of Georgia, Athens, Georgia, United States
[8]Department of Ophthalmology and Visual Sciences, Chinese University of Hong Kong, Hong Kong
[9]Joint Shantou International Eye Center, Shantou University and the Chinese University of Hong Kong, Shantou, China
[10]Department of Biochemistry and Molecular Biology, Indiana University School of Medicine Lafayette, West Lafayette, Indiana, United States
[11]Purdue Institute for Integrative Neuroscience, Purdue University, West Lafayette, Indiana, United States
[12]Purdue Institute for Drug Discovery, Purdue University, West Lafayette, Indiana, United States

Correspondence: Mingzhi Zhang, Joint Shantou International Eye Center, Dong Xia North Road, Shantou, 515041, Guangdong Province, China;
zmz@jsiec.org.
Yuk Fai Leung, Department of Biological Sciences, Purdue University, 915 W. State Street, West Lafayette, IN, 47907, USA;
yfleung@purdue.edu.

PV and IMH are co–first authors.

Current affiliations: *Department of Pharmacology, University of Michigan, Ann Arbor, Michigan, United States.
†Department of Chemistry and Food Science, Framingham State University, Framingham, Massachusetts, United States.
‡Epigenomics Core, University of Michigan, Ann Arbor, Michigan, United States.

**PURPOSE.** Although zebrafish rods begin to develop as early as 2 days postfertilization (dpf), they are not deemed anatomically mature and functional until 15 to 21 dpf. A recent study detected a small electroretinogram (ERG) from rods in a cone mutant called *no optokinetic response f* (*nof*) at 5 dpf, suggesting that young rods are functional. Whether they can mediate behavioral responses in larvae is unknown.

**METHODS.** We first confirmed rod function by measuring *nof* ERGs under photopic and scotopic illumination at 6 dpf. We evaluated the role of rods in visual behaviors using two different assays: the visual-motor response (VMR) and optokinetic response (OKR). We measured responses from wild-type (WT) larvae and *nof* mutants under photopic and scotopic illuminations at 6 dpf.

**RESULTS.** *Nof* mutants lacked a photopic ERG. However, after prolonged dark adaptation, they displayed scotopic ERGs. Compared with WT larvae, the *nof* mutants displayed reduced VMRs. The VMR difference during light onset gradually diminished with decreased illumination and became nearly identical at lower light intensities. Additionally, light-adapted *nof* mutants did not display an OKR, whereas dark-adapted *nof* mutants displayed scotopic OKRs.

**CONCLUSIONS.** Because the *nof* mutants lacked a photopic ERG but displayed scotopic ERGs after dark adaptation, the mutants clearly had functional rods. WT larvae and the *nof* mutants displayed comparable scotopic light-On VMRs and scotopic OKRs after dark adaptation, suggesting that these responses were driven primarily by rods. Together, these observations indicate that rods contribute to zebrafish visual behaviors as early as 6 dpf.

Keywords: zebrafish, visual motor response, optokinetic response, rods, electroretinogram

In the zebrafish eye, progenitor cells mainly withdraw from the cell cycle at 48 hours postfertilization (hpf) to form photoreceptor precursors in the outer nuclear layer of the retina.[1] Some of these precursors begin to differentiate into rods at 36 to 50 hpf in a specialized ventral patch region of the retina. They form outer segments and express *rhodopsin* (*rho*).[2–5] Subsequently, rods slowly increase in numbers throughout the retina.[4,6] Their synaptic terminals can be detected at approximately 62 hpf.[4,7] By 68 hpf, the retina is mature enough to initiate a visually evoked startle response.[8] Shortly after 72 hpf, the larvae also display an optokinetic response (OKR)[8] and an electroretinogram

(ERG).[9] Even though rods initially differentiate at early developmental stages, their role in mediating vision and visual behaviors has been controversial. For example, rods were deemed not anatomically mature until 15 to 20 days postfertilization (dpf), and not contributing to vision until this stage.[5] The first detectable physiological rod response by ERG recordings was also reported to appear between 15 and 21 dpf.[10] This uncertainty in rod function during early development has somewhat limited the utility of the zebrafish model for studying rod diseases and behavior.

Because the earlier ERG studies were performed in wild-type (WT) zebrafish, it is possible that rod responses might have been obscured by cone responses, which dominate early visual responses. To circumvent this issue, a recent study isolated rod responses in larvae as early as 5 dpf[11] by measuring ERGs in a cone mutant called *no optokinetic response f (nof)*. The *nof* mutant carries a point mutation, which introduces a premature stop codon in *gnat2 (guanine nucleotide binding protein [G protein], alpha transducing activity polypeptide 2)*, a gene encoding the alpha subunit of cone transducin.[12] This mutation leads to undetectable transducin protein in the *nof* retina up to 2 months of age. Even though the transducin is undetectable in *nof* retina, retinal morphology appears normal. The *nof* mutation also does not cause a secondary effect in the phototransduction pathway as evidenced by normal levels of opsins and RGS9 (regulator of G protein signaling 9), and normal activity of phosphodiesterase and guanylyl cyclase. The *nof* mutation, however, greatly affects cone function.[12] For example, with normal photopic light stimuli ($4.41 \times 10^4$ photons/$\mu m^2$ at 590 nm for 10 ms), no electrophysiological responses can be elicited from *nof* cones at 2 to 3.5 months. However, with very bright lights ($1.3 \times 10^7$ photons/$\mu m^2$/s at 590 nm for 2 s), it is possible to elicit a small, slow response from some *nof* cones that appears to result from the release of $Ca^{2+}$ into the cell cytoplasm from internal stores. These observations indicate that *nof* cones in young adults do not respond to normal photopic illumination. However, *nof* rods appear unaffected by the mutation and remain functionally intact. For example, single *nof* rods at 2 to 3.5 months have normal light sensitivity to 10-ms flashes compared with WT rods, suggesting their responses are not altered by the absence of functional cones. Using the *nof* mutant, rod function has been detected in zebrafish larvae as early as 5 dpf.[11] In that study, Moyano et al.[11] evaluated the effects of nicotine on cone and rod b-waves in the ERG. They detected small a- and b-wave responses from dark-adapted *nof* larvae at 5 dpf under scotopic illumination. These observations suggest that rods in young larvae are functional and contribute to the ERG. Nonetheless, it is not known whether these young rods contribute to visual behavioral responses. In this study, we first measured ERGs under both photopic and scotopic illumination in WT and *nof* mutants at 6 dpf to confirm rod function in young larvae. We found *nof* mutants lacked a photopic ERG, indicating that they lacked cone function. However, after dark adaptation, these mutants displayed scotopic ERGs over 5 log units of light attenuation. This indicates that their rods were functional at this stage.

We then tested the role of rods in driving visual behaviors of young zebrafish larvae with two different assays: the visual-motor response (VMR) and OKR. The VMR is a visual startle response displayed by zebrafish larvae with normal vision at both light onset (light-On) and offset (light-Off).[13,14] It can be detected in WT larvae as early as 3 dpf.[15] This response has been used by us and others to study the effect of mutations,[16–19] toxic chemicals,[20] and therapeutic

compounds on zebrafish vision.[17] It has also been used by us to evaluate the difference in response between different WT strains.[15,21,22] In a typical VMR assay, zebrafish larvae are presented with a series of light-On and light-Off stimuli. Each light-On stimulus is preceded by a dark phase, during which rods are dark-adapted for the upcoming light onset. Similarly, each light-Off stimulus is preceded by a light phase, during which rod responses are reduced or saturated, depending on the intensity of light illumination. A complication regarding the VMR is that extraocular photoreceptors (EOPs) found in hypothalamus and pineal gland can contribute to the response, especially when bright lights are used.[14,23] However, the EOP contribution to the VMR has a delayed onset and never shows the sharp initial peak characteristic of both the light-On and light-Off responses.[16,23] The EOP contribution can be differentiated from the photoreceptor contribution by analyzing the early phase of the VMR in the first few seconds, and by comparing the response with that obtained from an eyeless *chokh/rx3* mutant,[24] which only possesses EOPs but not ocular photoreceptors.

The OKR is a visual behavior triggered in normal WT larvae by a rotating drum with stripe gratings.[8,25,26] Each OKR consists of a smooth eye movement along the direction of drum rotation followed by a rapid saccade back. It can be detected in zebrafish larvae as early as 3 dpf and robustly starting at 5 dpf. The VMR and OKR comprise key visual responses in zebrafish larvae and are well suited for evaluating rod contribution to larval visual function. In this study, we optimized these visual behaviors for measuring rod response in zebrafish larvae. We also used the *nof* mutants to isolate rod function. We found that the *nof* mutants displayed a VMR and OKR as early as 6 dpf under scotopic conditions. Therefore rods likely contribute to visual behaviors in young zebrafish larvae.

## MATERIALS AND METHODS

### Fish Maintenance and Breeding

Adult fish were maintained according to standard procedures in a 14/10-hour light/dark cycle in the fish facility.[27–29] The *nof/gnat2^{w21}* (*nof*) mutant line[12] was obtained from Susan Brockerhoff at the University of Washington. The homozygous mutant embryos were obtained by crossing heterozygous parents because the mutants do not survive to adulthood. The control embryos were obtained from the genotyped WT siblings of the heterozygous parents. The *nof* mutants were identified at 5 dpf using the OKR. The *chokh/rx3* mutant line[24] was obtained from Jessica Miller at Harvard University. Their homozygous embryos do not develop eyes due to a mutation in the Rx3 homeodomain-containing transcription factor. They were obtained by crossing heterozygous parents. Because the *chokh/rx3* mutants lack eyes, they were easily identified at 2 dpf by morphologic observation. All embryos and larvae were raised in E3 medium[28] in a 28°C incubator with a 14/10 hour light/dark cycle. They were inspected and medium replaced every day. Unhealthy embryos were discarded and not used for any experiment. All protocols were approved by Purdue Animal Care and Use Committee and adhered to the ARVO statement for the Use of Animals in Ophthalmic and Vision Research.

### OKR Assay

In this study, a custom-made OKR apparatus was used based on the basic specifications previously reported.[25] To conduct

## A. OKR+

500 μV

500 ms

b-wave

a-wave

d-wave

## B. OKR- (*nof*)
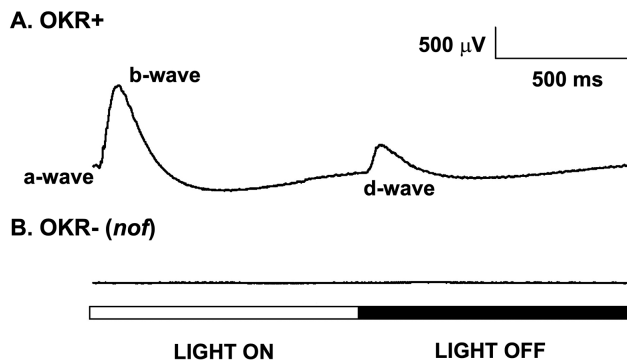
LIGHT ON          LIGHT OFF

**FIGURE 1.** Photopic ERG of WT and *nof* mutant larvae at 6 dpf. (**A**) ERGs of 6-dpf larvae that displayed OKR (WT phenotype; OKR+). (**B**) ERGs of 6-dpf OKR- (*nof*) larvae. All samples were adapted to light at 200 μW/cm$^2$ at 500 nm for at least 2 hours before the experiments. The light stimulus was a 500-ms full-field light flash of $5.3 \times 10^4$ μW/cm$^2$ at 500 nm (log $I = 0$). Each trace is an average of six responses. The *nof* mutants did not display any ERG under photopic conditions.

OKR measurements, the larvae were partially immobilized in 3% methylcellulose in a 35-mm Petri dish. The dish was placed in the center of a circular drum with 20° black and white vertical stripes attached on the inner surface. The stripes were illuminated by a Fiber Lite M1-150 illuminator (Dolan-Jenner Industries, Boxborough, MA, USA). Light intensity was measured by a Thorlabs PM100 optical power meter (Thorlabs, Newton, NJ, USA). Without attenuation (log $I = 0$), the irradiance was $1.1 \times 10^3$ μW/cm$^2$ at 500 nm at the level of Petri dish. To achieve lower light intensities, neutral-density filters were placed in the light path to attenuate the light. During OKR measurements, the rotation speed of the drum was set at three to four revolutions per minute. In response to such stripe rotation, normal larvae displayed characteristic OKR eye movements, including smooth pursuits and saccades.[25]

### ERG Recording

ERGs were recorded from isolated larval eyes as described.[30] The eyes were maintained in Ringer's solution that flowed continuously over the preparation and was maintained at pH 7.8 by gassing the solution by 97% $O_2$ and 3% $CO_2$.[16] The glass recording electrode had an 8- to 12-μm tip and contained a chloride-coated silver wire. The electrode was filled with Ringer's solution and inserted into the anterior chamber to record the summed outer retinal cell responses. The reference electrode was placed in the agarose covering the preparation stage. A 500-ms full-field light flash was used under photopic lighting condition to ensure b- and d-wave separation, whereas a 200-ms flash was used under scotopic conditions because no d-wave is elicited under these conditions. For photopic conditions, zebrafish larvae were adapted to light at approximately 200 μW/cm$^2$ at 500 nm for at least 2 hours. For scotopic recordings, animals were dark-adapted for at least 2 hours, followed by the eye preparation using dim red light at 670 nm under a dissecting microscope fitted with infrared light intensifiers. The stimulus light source was a 100W halogen bulb with a light intensity of $5.3 \times 10^4$ μW/cm$^2$ at 500 nm (log $I = 0$). Light was attenuated using Wratten neutral-density filters. Light readings were determined using Thorlabs PM100 optical power meter (Thorlabs). The ERG response was amplified, and low-pass filtered at 300 Hz. At least three recordings were averaged to obtain an ERG trace. All recordings were acquired using the LabVIEW program (National Instruments, Austin, TX, USA). Data analyses were conducted using IGOR Pro (WaveMetrics, Portland, OR, USA) custom-made software.

### VMR Assay

The VMR assay was designed based on published reports.[13] Larvae were individually arranged in a 96-plate (Whatman 96-squarewell UNIPLATE, GE Healthcare Bio-Sciences, Marlborough, MA, USA) inside a ZebraBox system (ViewPoint Life Sciences, Lyon, France). They were isolated from environmental light and stimulated by white light emitted by a light source placed from the bottom of the 96-well plate. The larval movement was recorded by an infrared sensitive camera at a rate of 30 frames per second under 850-nm infrared illumination, not perceived by the larvae. Before experiments, larvae in the 96-well plate were dark-adapted in the ZebraBox system for 3.5 hours. The actual test consisted of three consecutive trials of light onset (light-On) and light offset (light-Off) periods, each period lasting for 30 minutes. In other words, the larvae were exposed to either light or dark for 30 minutes before the next light change. The light change (on or off) was abrupt and set at different light intensities. The light intensity was measured by an ILT950 spectroradiometer (International Light Technologies, Peabody, MA, USA) from each well of an empty 96-well plate placed on top of the light source. At the maximum output intensity (100%), the average irradiance at 500 nm was 3.77 μW/cm$^2$ ($SD = 0.54$) (log $I = 0$). Lower light intensities were achieved by adjusting the output light intensity of the Zebrabox by 2 log units (i.e., between 1% and 100%), and by adding neutral density filters (BarnDoor Lighting Outfitters, North Branford, CT, USA) in-between the light source and the 96-well plate. Each neutral density filter blocked approximately 60% of the light. The reduction in light intensity did not alter the color temperature. The following light intensities (log $I$) were used in the VMR experiments: 0, −0.2, −2.5, −2.9, and −3.3.

During the VMR assay, the larval activity was recorded by Zebralab software (View-Point Life Sciences) running in the quantification mode. The following parameters were used to collect activity data: detection sensitivity per pixel per image—gray level 6; burst threshold—4 pixels; bin size—1 second. The detection sensitivity registered pixels with a gray level below a preset level. These registered pixels detected the individual larvae in each frame. If these pixels were detected in a different location in successive frames, they were declared as active pixels. These active pixels represented the part of the larvae that moved in successive frames. The burst threshold selected movements that were larger than a predefined number of active pixels between successive frames to separate small movements from major movements. In this study, larval movement was summarized as the fraction of frames that a larva displayed movement in each second (as defined by the bin size). This fraction was defined as the Burst Duration and was individually computed for all larvae. All VMR assays were started at approximately the same time at 2 PM in the afternoon to minimize the effect of circadian rhythm on vision.[31] The media were changed every day. The larval genotype was confirmed by PCR after all behavioral experiments. In all experiments, three independent biological replicates were performed. Each biological replicate comprised three technical replicates.
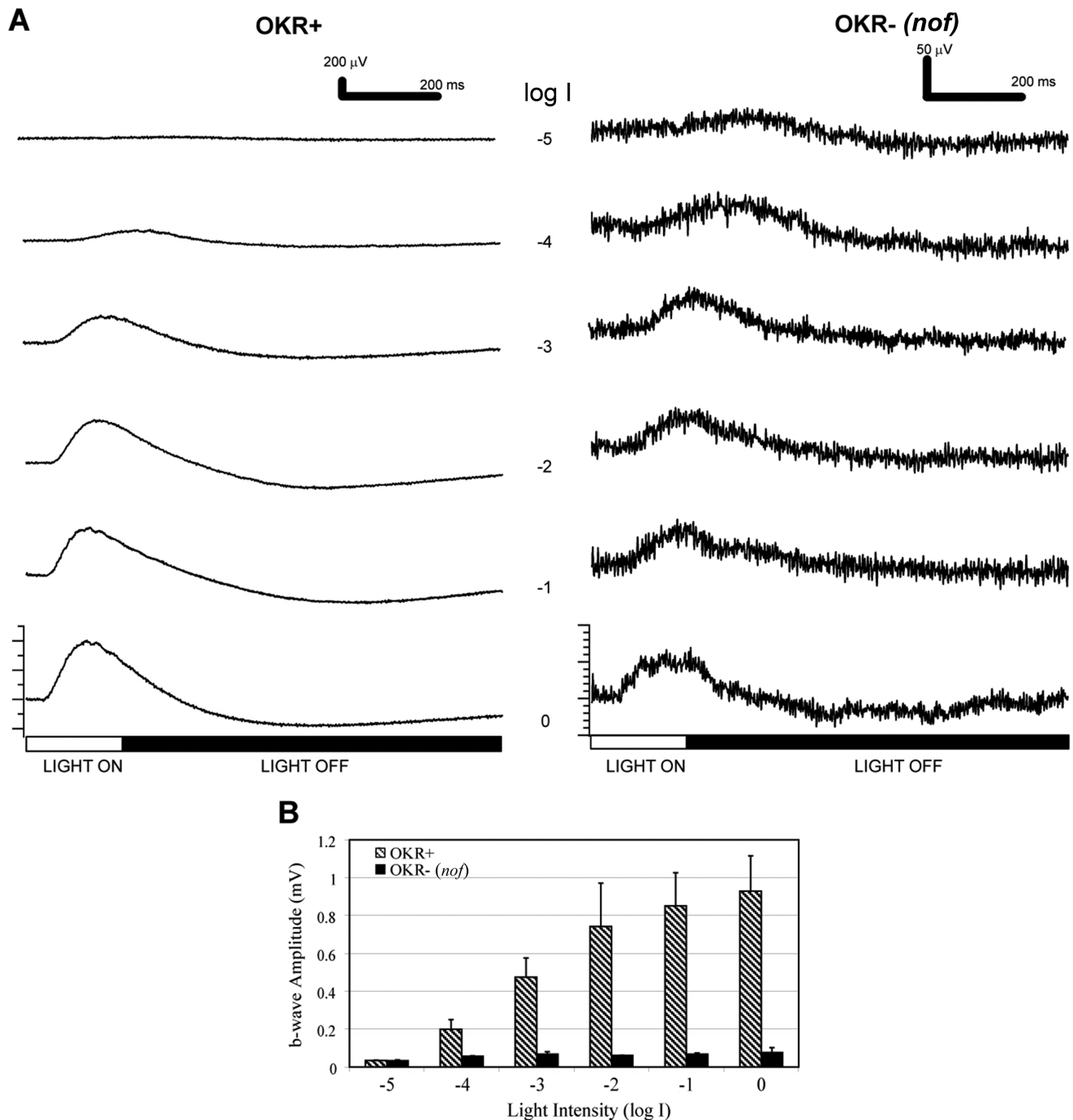
**FIGURE 2.** The *nof* mutants displayed scotopic ERGs after dark adaptation. (**A**) ERGs of OKR+ larvae (*left panel*) and OKR- larvae (*right panel*) over 5 log units of light attenuation. The unattenuated light stimulus was a 200-ms full-field light flash of $5.3 \times 10^4$ µW/cm$^2$ at 500 nm (log $I = 0$). Each trace is an average of three responses. (**B**) Bar graph indicating the b-wave amplitude averages of OKR+ ($n = 3$) and OKR- ($n = 3$) larvae over 5 log units of light attenuation. After dark adaptation, both OKR+ and OKR- (*nof*) larvae were responsive at dim light indicative of rod function.

## Genotyping

The OKR-negative *nof* larvae were genotyped after the VMR assay to confirm their homozygosity. Their DNA was extracted by the alkaline lysis method. Briefly, these larvae were heated to 95°C in 50 mM NaOH for 10 minutes in Eppendorf tubes. The solution was vortexed, neutralized with 1M Tris-HCl, and centrifuged at 18,400 g. The supernatant was used in PCR with the follow-ing primers: forward—5′-GGAGTTCATCGTGCCAAAAC-3′, reverse—5′-GTGTTTCAACTCACTTCAGCT-3′. The resulting PCR products were digested with PVU-II (New England Biolabs, Ipswich, MA, USA) and run on an agarose gel. The WT PCR product was cut by the enzyme into two bands: a 145 base pairs (bp) band and a 19-bp band, whereas the PCR product with the *nof* mutation was not cut by the enzyme and remained a 164-bp band.
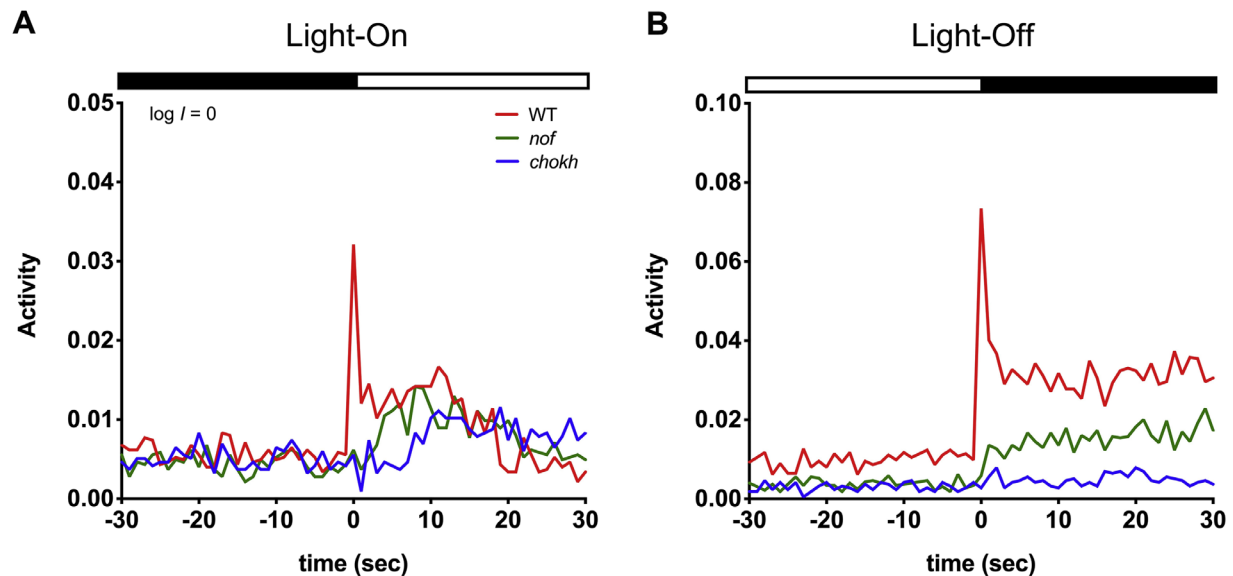
**FIGURE 3.** VMRs of WT larvae, *nof*, and *chokh/rx3* mutants at log $I = 0$. VMRs recorded from WT larvae (*red*; $N = 108$), *nof* (*green*; $N = 108$), and *chokh/rx3* mutants (*blue*; $n = 72$) at 6 dpf with a light stimulus of log $I = 0$ (3.77 µW/cm² at 500 nm). Activity is the fraction of video frames in which a larva displayed movement each second (see Methods). In each plot, the curves show the average activity of the larvae in each condition. The light and dark phases are shown by white and black bars respectively, at the top of the plots. (**A**) Light-On VMRs. The *nof* and *chokh/rx3* mutants lacked the fast response (<2 s after light onset) that the WT larvae displayed. All larvae displayed a gradual increase in sustained activity (>2 s after light onset), although the sustained amplitudes of both mutants were considerably smaller than that of WT larvae. (**B**) Light-Off VMRs. The *nof* mutants displayed a severe reduction in amplitude of the fast response (<2 s after light offset) compared with that of the WT larvae. All larvae displayed a sustained response (>2 s after light offset), with WT larvae the highest and *chokh/rx3* mutants the lowest.

## Statistics

Statistical analysis was performed using R version 3.3.0 <https://www.r-project.org/>. VMR data were processed by DataWorkShop (ViewPoint Life Sciences) to extract locomotor activity after each stimulus change. To compare activity profiles, the locomotor activity from different conditions was segregated into two time periods: 1 to 2 seconds (fast response) and 3 to 10 seconds (sustained response). The activity profiles in these time periods were compared by the Hotelling's T² test, a statistical approach we developed to analyze VMR data.[15] Finally, the resulting *P* values were corrected for multiple-hypothesis testing by controlling the false-discovery rate.

## Relative Activity

The relative activity between two samples was expressed as a ratio percentage between their areas under the curve (AUC). Two time periods were used in the calculation: 0 to 2 seconds and 2 to 10 seconds. The former period includes the activities used in the statistical analysis of the fast response (the first 2 seconds) as described in the last section, whereas the later period includes the activities used in the statistical analysis of the sustained response (3–10 seconds). In the Results section, the time periods for AUC calculation would be grouped under the fast and sustained responses used in the statistical analysis for clarity.

## RESULTS

### The *nof* Mutation Inactivated Cone Function But Not Rod Function

We first confirmed the lack of cone function in the *nof* mutants by ERG measurements (Fig. 1). The mutant larvae were identified by their lack of an OKR at 5 dpf (OKR−). Their ERGs were measured under photopic condition (5.3 × 10⁴ µW/cm² at 500 nm; log $I = 0$) at 6 dpf and compared with those obtained from WT siblings (OKR+). The OKR+ larvae displayed ERGs that consist of three typical components (Fig. 1A): a small initial a-wave during light onset that represents the hyperpolarization of photoreceptors, a depolarizing b-wave that reflects ON-bipolar cell activity, and a depolarizing d-wave during light offset that reflects OFF-bipolar cell activity[30,32] driven by cones. The OKR− (*nof*) larvae, on the contrary, did not display any ERGs under normal photopic conditions (Fig. 1B).

To measure potential rod function, the ERGs of these larvae after 2-hour dark adaptation were measured over 5 log units of light intensities (Fig. 2). In this preparation, both OKR+ and OKR- larvae displayed ERGs (Fig. 2A). The OKR- ERG was much smaller than the OKR+ ERG at all intensities, except for log $I = -5$. At this light intensity, the b-wave amplitudes were comparable between OKR- larvae and OKR+ larvae, in both cases approximately 33 µV (Fig. 2B). As the light intensity increased, the b-wave amplitudes of the OKR+ larvae increased substantially, whereas those of the OKR- larvae remained in the range of 30 to 70 µV.

### VMRs in WT Larvae and *nof* Mutants

We then determined the extent to which the VMR was altered by the *nof* mutation by comparing the VMRs displayed by WT larvae and *nof* mutants at 6 to 8 dpf. The results from each stage were consistent, and the 6-dpf results are presented here unless otherwise specified. At log $I = 0$ (3.77 µW/cm² at 500 nm), the WT larvae displayed a characteristic fast, transient light-On response in the first two seconds (fast response) (Fig. 3A). They also displayed a
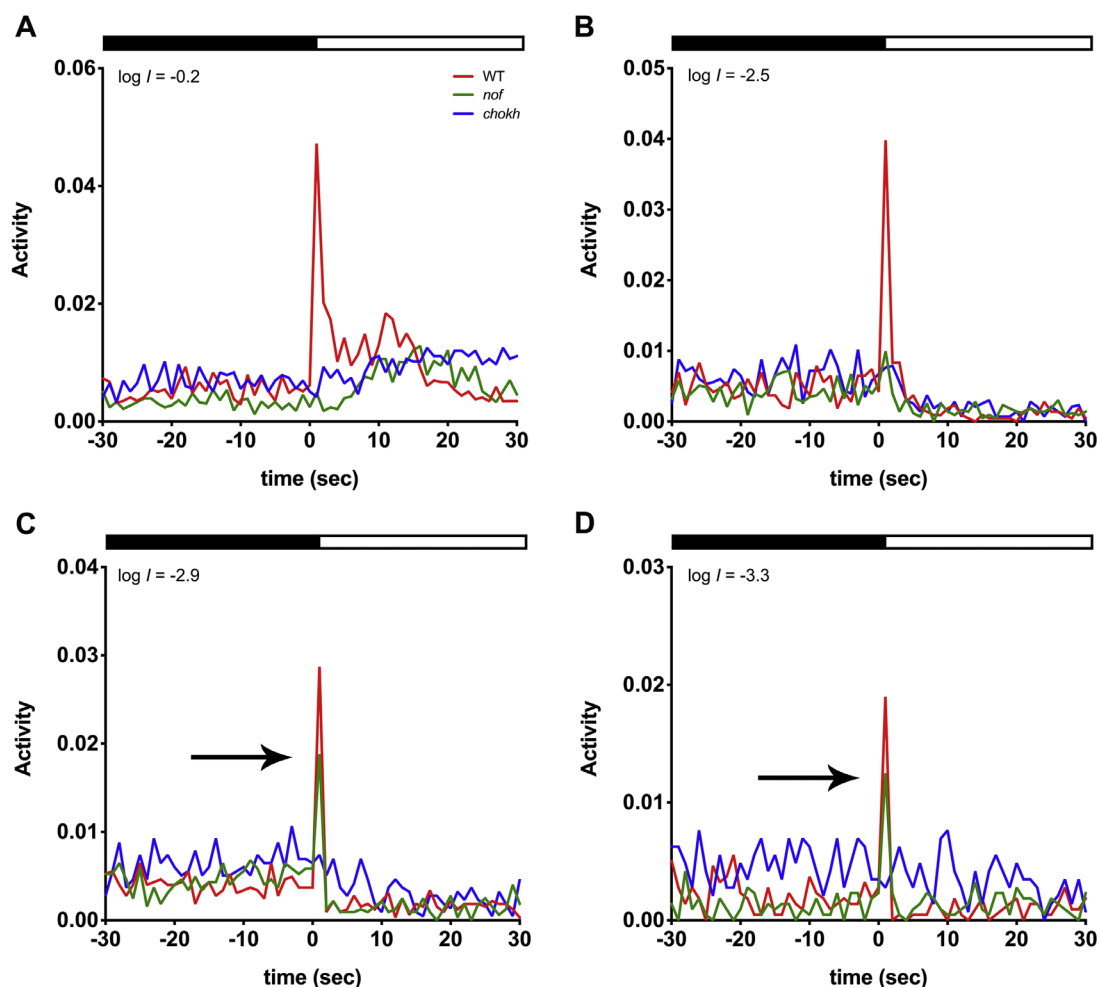
**FIGURE 4.** The *nof* mutants displayed a light-On VMR comparable to that of WT larvae at the lowest light intensities (log $I = -2.9$ and $-3.3$). The light-On VMRs of WT larvae (*red*), *nof* (*green*), and *chokh/rx3* mutants (*blue*) were measured at 6 dpf with the following light intensities: log $I = -0.2$ (**A**), $-2.5$ (**B**), $-2.9$ (**C**), and $-3.3$ (**D**). The experiments were conducted and resulting data plotted as described in Figure 3. The numbers of animals used are as follows: For (**A**, **B**), $n = 72$ for WT larvae and *nof* mutants, and $n = 48$ for *chokh/rx3* mutants; for (**C**), $n = 108$ for WT larvae and *nof* mutants, and $n = 72$ for *chokh/rx3* mutants; for (**D**), $n = 36$ for WT larvae and *nof* mutants, and $n = 24$ for *chokh/rx3* mutants. As the light intensity was reduced, WT larvae and the *nof* mutants displayed fast responses (<2 s after light onset) that became more comparable. The *arrows* in (**C**, **D**) indicate WT and *nof* mutants displayed a similar fast response in the first 2 s. The *chokh/rx3* mutants, however, did not display any fast response. All larvae lacked sustained responses (>2 s after light onset) when the stimulus light intensity was lower than log $I = -2.5$.

sustained response, which consisted of a few peaks starting from the third second and which lasted for almost 30 seconds. Compared with the WT larvae, the *nof* mutants displayed a significantly different light-On VMR (Fig. 3A). It lacked the sharp activity peak of the fast response ($P < 0.0001$), and responded, but was slightly less active during the sustained response (3–10s, 82%, $P < 0.08$). Nonetheless, a few activity peaks were still apparent. During light offset, the WT larvae displayed a characteristic fast, transient light-Off VMR in the first 2 seconds (fast response), and a sustained response with multiple peaks that lasted for several minutes before the activity returned to baseline (Fig. 3B). Compared with the WT larvae, the *nof* mutants also showed a different light-Off VMR (Fig. 3B) that lacked most of the sharp activity peak of the fast response ($P < 0.0001$), and their sustained response was also significantly reduced (3–10s, 44%, $P < 0.0001$).

The contribution of the EOPs to the VMR at 6 dpf was evaluated by measuring VMRs displayed by the eyeless *chokh/rx3* mutants (Figs. 3A, 3B). On light onset, the *chokh/rx3* mutants completely lacked the fast response of the first 2 seconds but they gradually increased their activity from 7 seconds onward (Fig. 3A). During this sustained period, a few activity peaks occurred every few seconds. On light offset, the *chokh/rx3* mutants barely displayed any light-Off VMR (Fig. 3B), except perhaps for a small fast off-response.

## The Light-On VMR of the *nof* Mutants at Lower Light Intensities Resembles the WT Response

To evaluate a contribution of rods to the VMR, we lowered the intensity of the light stimuli to levels that would only
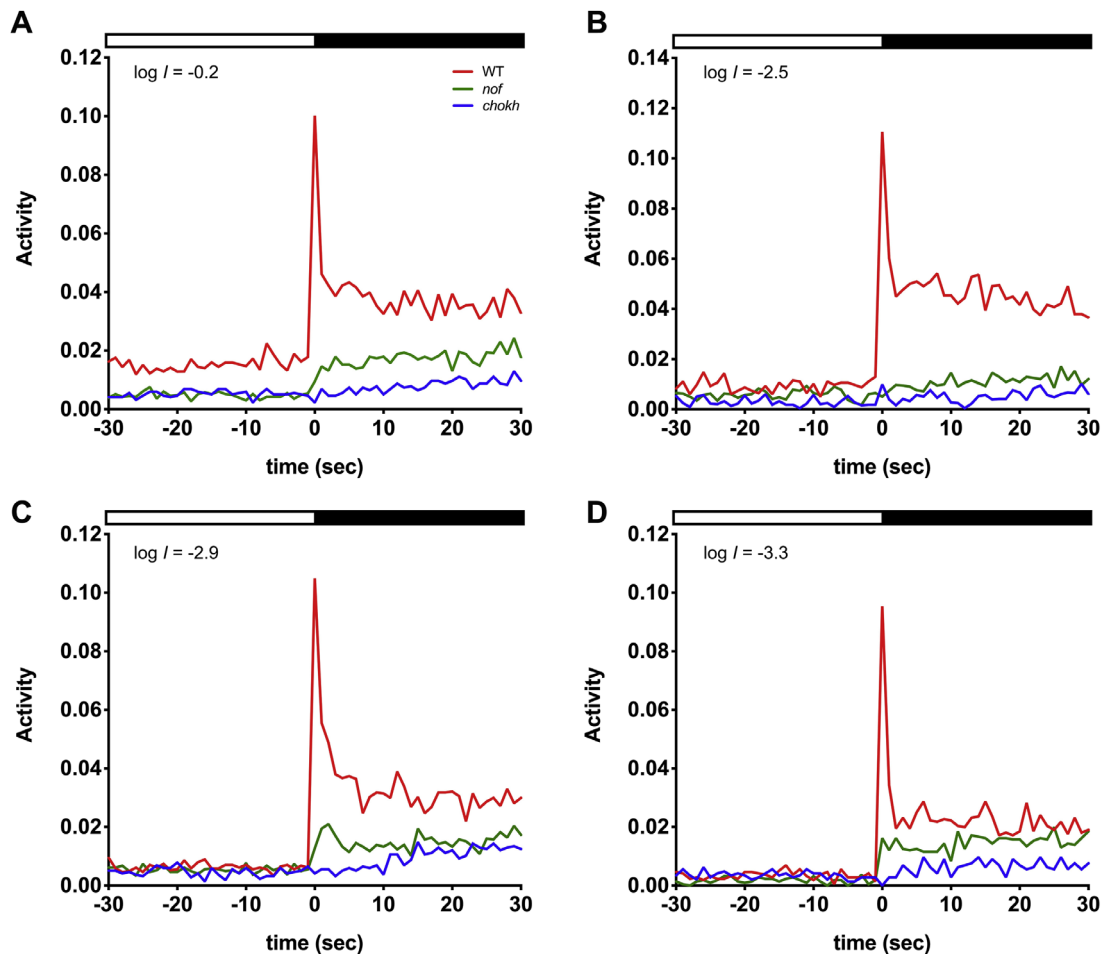
**FIGURE 5.** The *nof* mutants displayed a reduced light-Off VMR, which was still higher than that of the *chokh/rx3* mutants at low-light intensities. The light-Off VMRs of WT larvae (*red*), *nof* (*green*), and *chokh/rx3* mutants (*blue*) were measured at 6 dpf with the following light intensities: $\log I = -0.2$ (**A**), $-2.5$ (**B**), $-2.9$ (**C**), and $-3.3$ (**D**). The experiments were conducted and resulting data plotted as described in Figure 3. The numbers of animals used are as follows: For (**A**, **B**), $n = 72$ for WT larvae and *nof* mutants, and $n = 48$ for *chokh/rx3* mutants; for (**C**), $n = 108$ for WT larvae and *nof* mutants, and $n = 72$ for *chokh/rx3* mutants; for (**D**), $n = 36$ for WT larvae and *nof* mutants, and $n = 24$ for *chokh/rx3* mutants. Compared with WT larvae, the *nof* mutants always showed a reduction in amplitude of the fast response ($<2$ s after light offset). The sustained responses ($>2$ s after light offset) were also noticeably less. Nonetheless, the responses from the *nof* mutants were generally higher than the ones displayed by the *chokh/rx3* mutants.

activate rods. In that case, WT larvae and the *nof* mutants should display similar light-On VMRs. To test this, we systematically subjected WT larvae, *nof* and *chokh/rx3* mutants to lower light intensities and measured their light-On VMRs (Figs. 4A–D).

At $\log I = -0.2$, the *nof* mutants did not display any fast response (Fig. 4A). A small fast peak was detected at $\log I = -2.5$ (Fig. 4B), but it was substantially smaller than the WT response (30%; $P < 0.0001$). However, at $\log I = -2.9$ and $-3.3$, the *nof* mutants displayed fast responses similar to WT larvae (72% and 91%, $P > 0.05$) (Figs. 4C, 4D). However, the *chokh/rx3* mutants displayed no fast response when exposed to light intensities lower than $\log I = 0.2$. Indeed, at light intensities below $\log I = -2.5$, there was a suppression of activity of all sustained responses. The same trend persisted at 8 dpf, except for *nof* mutants that started to display a small fast response at $\log I = -0.2$ ($<50\%$ of WT; $P < 0.004$).

## Rods Contribute to the Light-Off VMR in Zebrafish Larvae

The *nof* mutants displayed a substantially reduced light-Off VMR compared with WT larvae at all lower light intensities (Figs. 5 A–D). They lacked any fast response at $\log I = -0.2$ and $-2.5$ but did display a small peak of less than 30% of WT amplitude at $\log I = -2.9$ and $-3.3$ ($P < 0.0001$), which *chokh/rx3* mutants did not display. The *nof* mutants also displayed some small, sustained responses that were greater than the responses of the *chokh/rx3* mutants ($<52\%$ of *nof* mutants) at all light intensities ($P < 0.041$).

## Rods Also Contribute to the OKR in Zebrafish Larvae

We measured the OKR of *nof* mutants and their WT siblings at 6 dpf over 5 log units of light attenuation (At $\log I = 0$, the irradiance was $1.1 \times 10^3$ µW/cm$^2$ at 500 nm). When
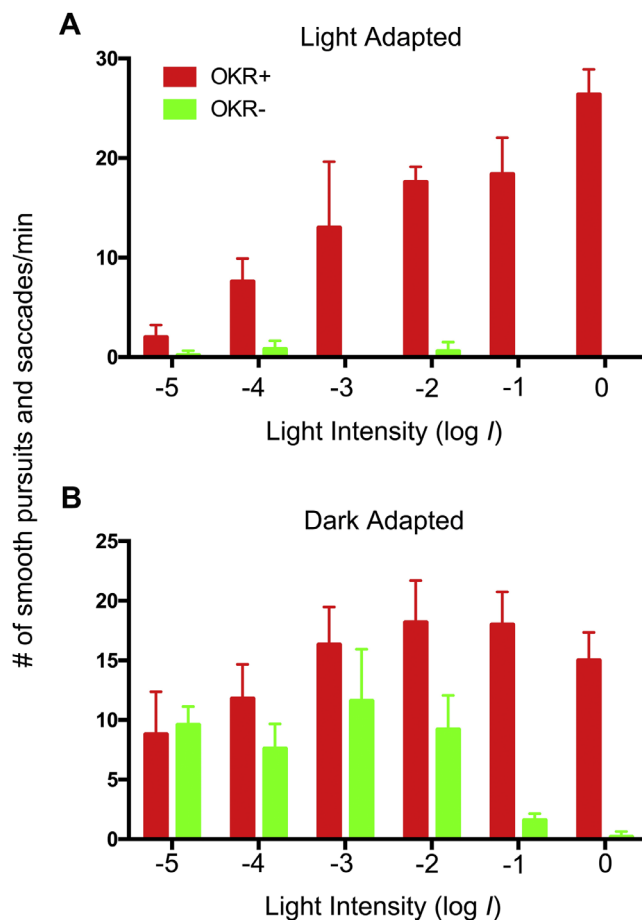
**A** Light Adapted

**B** Dark Adapted

**FIGURE 6.** Dark-adapted *nof* mutants displayed an OKR at low-light intensities. In this experiment, heterozygous *nof* parents were crossed. At 5 dpf, the OKRs of the collected larvae were tested under photopic condition to identify WT larvae (OKR+, $n = 10$) and *nof* mutants (OKR−, $n = 10$). At 6 dpf, these larvae were light-adapted at 200 µW/cm² at 500 nm (**A**) or dark-adapted (**B**) for 2 hours and their OKRs tested over 5 log units of attenuated light (log $I = 0$; $1.1 \times 10^3$ µW/cm² at 500 nm). The bar charts show the average number of smooth pursuits and saccades per minute as a function of light intensity. The *error bars* show the standard deviations. The *nof* mutants displayed an OKR comparable with the WT larvae at log $I = -3$ or less.

*nof* mutants were light-adapted (200 µW/cm² at 500 nm for 2 hours), a few sporadic smooth pursuits and saccades were recorded at lower light-stimulus intensities. Nonetheless, the mutants did not display any consistent and continuous OKR compared with their WT counterparts, which displayed an OKR with the number of smooth pursuits and saccades per minute correlating with the light-stimulus intensity (Fig. 5A; $P < 0.05$ for all intensities). The *nof* mutants did display an OKR when they were dark-adapted before the assay (Fig. 5B). When the light intensity was equal to or lower than log $I = -3$, the *nof* mutants displayed an OKR indistinguishable from the WT siblings ($P > 0.05$). At higher light intensities from log $I = -2$ to 0, the *nof* mutants displayed fewer smooth pursuits and saccades per minute ($P < 0.05$).

## DISCUSSION

Our ERG measurements unequivocally demonstrated rod responses from the *nof* mutant. First, light-stimulus intensities at or below log $I = -4$ (5.3 µW/cm² for 200 ms or 1.06 µJ/cm²) (Fig. 2) are comparable or less than those that Brockerhoff et al.[12] used and failed to trigger a response from isolated *nof* cones (a 10-ms flash of $4.41 \times 10^4$ photons/µm², which is equivalent to 148.3 µW/cm² for 10 ms or 1.48 µJ/cm²). Although some of the isolated *nof* cones do respond to very bright light through a transducin-independent increase of cytoplasmic Ca²⁺, the stimulus intensity was far higher ($1.3 \times 10^7$ photons/µm²/s for 2 s, which is equivalent to 437.2 µW/cm² for 2 s or 874.3 µJ/cm²) than our scotopic light-stimulus intensities. This high level of light stimulus is comparable to our log $I = -1$ (Fig. 2). Together, these results indicate that our scotopic light-stimulus intensities (at or below log $I = -4$) could not have stimulated any Ca²⁺-dependent response from *nof* cones, and that the observed *nof* ERGs at these intensities were initiated by *nof* rods. The rod response in larvae was, however, relatively small, most likely due to far fewer rods being present in the larval retinas compared with the adult.[33] This small rod response was likely obscured by the dominating cone activity in the WT larvae, explaining why the earlier ERG studies did not detect rod response at these young ages.[10]

Because young zebrafish rods display electrophysiological responses, could they drive visual behaviors? Our study tested this possibility by VMR and OKR behavioral responses. If rods contribute to the VMR, we would expect to see differences between the responses of WT larvae, *nof* mutants with rod but no normal cone function, and eyeless *chokh* mutants. Indeed, the *nof* mutants displayed attenuated light-On and light-Off VMRs compared with WT larvae, but their VMRs were still higher than those displayed by the *chokh/rx3* mutants (Fig. 3). We included the eyeless *chokh/rx3* mutants[24] in these studies to eliminate the possibility of a confounding response originating from the EOPs. These EOPs do contribute a bit to the VMR, which is apparent when the results are summarized in minutes.[14,23] Although our results are summarized in seconds, we can still see some delayed responses by the *chokh/rx3* mutants from approximately 5 to 30 s in the light-On VMR at log $I = 0$ and −0.2, and in the light-Off VMR at all intensities (Figs. 3 and 4). Because all types of samples displayed regular activity peaks in the sustained period in light-Off VMR, these activity peaks likely have other extraocular origins.

Rod function was also demonstrated by the comparisons of VMRs at scotopic light intensities. At or below log $I = -2.9$ (0.0049 µW/cm²), only WT and *nof* mutants displayed the fast response in the light-On VMR (Fig. 4), whereas no fast responses were detected in the eyeless *chokh/rx3* mutants. These results indicate that EOPs were incapable of initiating the light-On VMR below log $I = -2.9$ and that the fast response of the *nof* mutants was likely driven by rods. At higher light intensities, WT larvae displayed a larger fast response compared with *nof* mutants, suggesting that cones mainly generate the WT fast response at these higher light intensities. The sustained response of light-On VMRs in all samples was largely reduced to the baseline level at or below log $I = -2.5$, suggesting that this component was primarily driven by cones. For light-Off VMR, the *nof* mutants displayed a small activity peak in the fast response (Figs. 4C, 4D), which was higher than the eyeless *chokh/rx3* mutants, but lower than the WT larvae (with rods and cones). This fast response likely represents rod contribution to the light-Off VMR. For the sustained response of the

light-Off VMR, the *nof* mutants always displayed activities lower than the WT larvae and higher than the *chokh/rx3* mutants, again indicating rods' contribution to the sustained activity. Together, our results strongly suggest that rods contribute to both the light-On and light-Off VMR in young larvae at 6 dpf.

Rod function was further demonstrated in the OKR that evaluates larval capability of tracking moving objects. Light-adapted *nof* mutants displayed little if any OKR, suggesting the light adaptation saturated their rods (Fig. 5A). Dark-adapted *nof* mutants, however, displayed OKRs across different light intensities (Fig. 5B). In particular, their OKRs were similar to those displayed by their WT siblings when the light intensity was lower than $\log I = -3$ (1.1 µW/cm$^2$). This light intensity is comparable to the scotopic light intensities used for rod ERG measurement ($< \log I = 4$, or 5.3 µW/cm$^2$ for 200 ms). This again indicates that rods were driving *nof* OKR at these lower light intensities. At higher light intensities, the *nof* mutants displayed smaller OKR responses, consistent with the notion that the stronger light intensities saturate the rods, diminishing the response.

## CONCLUSIONS

We have detected rod function and contributions to both the VMR and OKR in zebrafish larvae as early as 6 dpf. This observation has opened up the possibility of testing new drugs for rod degeneration in zebrafish.[14] We can screen compounds that improve the VMR in rod mutants, as the VMR is amenable to high-throughput screening. In addition, we can use the OKR for a more detailed analysis of specific compounds. Because these behavioral assays detect functional output of rods, they can complement fluorescent-based screening,[34] (Zhang L, et al. *IOVS* 2017;58:ARVO E-Abstract 4539) that detects rod survival. Together, these screening approaches may expedite discovery of new treatments for retinal degenerations that affect rods.

Disclosure: **P. Venkatraman,** None; **I. Mills-Henry,** None; **K.R. Padmanabhan,** None; **P. Pascuzzi,** None; **M. Hassan,** None;

**J. Zhang,** None; **X. Zhang,** None; **P. Ma,** None; **C.P. Pang,** None; **J.E. Dowling,** None; **M. Zhang,** None; **Y.F. Leung,** None

## *References*

1. Hu M, Easter SS. Retinal neurogenesis: the formation of the initial central patch of postmitotic cells. *Dev Biol*. 1999;207:309–321.

2. Morris AC, Fadool JM. Studying rod photoreceptor development in zebrafish. *Physiol Behav*. 2005;86:306–313.

3. Hensley MR, Emran F, Bonilla S, et al. Cellular expression of Smarca4 (Brg1)-regulated genes in zebrafish retinas. *BMC Dev Biol*. 2011;11:45.

4. Schmitt EA, Dowling JE. Early retinal development in the zebrafish, Danio rerio: light and electron microscopic analyses. *J Comp Neurol*. 1999;404:515–536.

5. Branchek T, Bremiller R. The development of photoreceptors in the zebrafish, Brachydanio rerio. I. Structure. *J Comp Neurol*. 1984;224:107–115.

6. Fadool JM. Development of a rod photoreceptor mosaic revealed in transgenic zebrafish. *Dev Biol*. 2003;258:277–290.

7. Schmitt EA, Dowling JE. Early eye morphogenesis in the zebrafish, Brachydanio rerio. *J Comp Neurol*. 1994;344:532–542.

8. Easter SS, Nicola GN. The development of vision in the zebrafish (Danio rerio). *Dev Biol*. 1996;180:646–663.

9. Branchek T. The development of photoreceptors in the zebrafish, Brachydanio rerio. II. Function. *J Comp Neurol*. 1984;224:116–122.

10. Bilotta J, Saszik S, Sutherland SE. Rod contributions to the electroretinogram of the dark-adapted developing zebrafish. *Dev Dyn*. 2001;222:564–570.

11. Moyano M, Porteros A, Dowling JE. The effects of nicotine on cone and rod b-wave responses in larval zebrafish. *Vis Neurosci*. 2013;30:141–145.

12. Brockerhoff SE, Rieke F, Matthews HR, et al. Light stimulates a transducin-independent increase of cytoplasmic Ca2+ and suppression of current in cones from the zebrafish mutant nof. *J Neurosci*. 2003;23:470–480.

13. Emran F, Rihel J, Dowling JE. A behavioral assay to measure responsiveness of zebrafish to changes in light intensities. *J Vis Exp*. 2008;20:923.

14. Ganzen L, Venkatraman P, Pang CP, Leung YF, Zhang M. Utilizing zebrafish visual behaviors in drug screening for retinal degeneration. *Int J Mol Sci*. 2017;18(6):1185.

15. Liu Y, Carmer R, Zhang G, et al. Statistical analysis of zebrafish locomotor response. *PLoS One*. 2015;10:e0139521.

16. Emran F, Rihel J, Adolph AR, Wong KY, Kraves S, Dowling JE. OFF ganglion cells cannot drive the optokinetic reflex in zebrafish. *Proc Natl Acad Sci USA*. 2007;104:19126–19131.

17. Zhang L, Xiang L, Liu Y, et al. A naturally-derived compound Schisandrin B enhanced light sensation in the pde6c zebrafish model of retinal degeneration. *PLoS One*. 2016;11:e0149663.

18. Maurer CM, Schönthaler HB, Mueller KP, Neuhauss SCF. Distinct retinal deficits in a zebrafish pyruvate dehydrogenase-deficient mutant. *J Neurosci*. 2010;30:11962–11972.

19. Gao Y, Chan RHM, Chow TWS, et al. A high-throughput zebrafish screening method for visual mutants by light-induced locomotor response. *IEEE/ACM Trans Comput Biol Bioinforma*. 2014;11:693–701.

20. Deeti S, O'Farrell S, Kennedy BN. Early safety assessment of human oculotoxic drugs using the zebrafish visualmotor response. *J Pharmacol Toxicol Methods*. 2014;69:1–8.

21. Gao Y, Zhang G, Jelfs B, et al. Computational classification of different wild-type zebrafish strains based on their

variation in light-induced locomotor response. *Comput Biol Med*. 2016;69:1–9.

22. Liu Y, Ma P, Cassidy PA, et al. Statistical analysis of zebrafish locomotor behaviour by generalized linear mixed models. *Sci Rep*. 2017;7:2937.

23. Fernandes A, Fero K, Arrenberg A, Bergeron S, Driever W, Burgess H. Deep brain photoreceptors control light-seeking behavior in zebrafish larvae. *Curr Biol*. 2012;22:2032–2047.

24. Loosli F, Staub W, Finger-Baier KC, et al. Loss of eyes in zebrafish caused by mutation of chokh/rx3. *EMBO Rep*. 2003;4:894–899.

25. Brockerhoff SE. Measuring the optokinetic response of zebrafish larvae. *Nat Protoc*. 2006;1:2448–2451.

26. Brockerhoff SE, Hurley JB, Janssen-Bienhold U, Neuhauss SC, Driever W, Dowling JE. A behavioral screen for isolating zebrafish mutants with visual system defects. *Proc Natl Acad Sci U S A*. 1995;92:10545–10549.

27. Hensley MR, Leung YF. A convenient dry feed for raising zebrafish larvae. *Zebrafish*. 2010;7:219–231.

28. Nüsslein-Volhard C, Dahm R. *Zebrafish: A Practical Approach*. New York: Oxford University Press; 2002.

29. Westerfield M. *The Zebrafish Book: A Guide for the Laboratory Use of Zebrafish (Danio Rerio)*. Oregon: University of Oregon Press; 2007.

30. Wong KY, Gray J, Hayward CJC, Adolph AR, Dowling JE. Glutamatergic mechanisms in the outer retina of larval zebrafish: analysis of electroretinogram b- and d-waves using a novel preparation. *Zebrafish*. 2004;1:121–131.

31. Emran F, Rihel J, Adolph AR, Dowling JE. Zebrafish larvae lose vision at night. *Proc Natl Acad Sci U S A*. 2010;107:6034–6039.

32. Stockton RA, Slaughter MM. B-wave of the electroretinogram. A reflection of ON bipolar cell activity. *J Gen Physiol*. 1989;93:101–122.

33. Raymond PA, Colvin SM, Jabeen Z, et al. Patterning the cone mosaic array in zebrafish retina requires specification of ultraviolet-sensitive cones. *PLoS One*. 2014;9:e85325.

34. White DT, Eroglu AU, Wang G, et al. ARQiv-HTS, a versatile whole-organism screening platform enabling in vivo drug discovery at high-throughput rates. *Nat Protoc*. 2016;11:2432–2453.